Korean J. Chem. Eng., 38(1), 72-80 (2021)
DOI: 10.1007/s11814-020-0674-3

pISSN: 0256-1115
eISSN: 1975-7220

Microbial fuel cell for oilfield produced water treatment and reuse: Modelling and process optimization

Majid Mohammadi*, Mehdi Sedighi,†, Rajamohan Natarajan***, Sedky Hassan Aly Hassan****, and Mostafa Ghasemi***,†**

*Department of Energy Engineering, Qom University of Technology, Qom, Iran
**Division of Energy Systems, Department of Chemical Engineering, University of Qom, Qom, Iran
***Chemical Engineering Section, Sohar University, Sohar, 311, Oman
****Botany & Microbiology Department, Faculty of Science, New Valley University, 72511 El-Kharga, Egypt
(*Received 8 April 2020 • Revised 16 August 2020 • Accepted 6 September 2020*)

Abstract−Oilfield produced water is one of the vast amounts of wastewater that pollute the environment and cause serious problems. In this study, the produced water was treated in a microbial fuel cell (MFC), and response surface methodology and central composite design (RSM/CCD) were used as powerful tools to optimize the process. The results of two separate parameters of sulfonated poly ether ether ketone (SPEEK) as well as nanocomposite composition (CNT/Pt) on the chemical oxygen demand (COD) removal and power generation were discussed. The nanocomposite was analyzed using XRD, SEM, and TEM. Moreover, the degree of sulfonation (DS) was measured by NMR. A quadratic model was utilized to forecast the removal of COD and power generation under distinct circumstances. To obtain the maximum COD removal along with maximum power generation, favorable conditions were achieved by statistical and mathematical techniques. The findings proved that MFC could remove 92% of COD and generate 545 mW/m^2 of power density at optimum conditions of DS=80; and CNT/Pt of 14 wt% CNT- 86 wt% Pt.

Keywords: MFC, COD Removal, Power Generation, CNT/Pt Nanocomposite, Optimization

INTRODUCTION

The oil and gas industry is developing quickly and water plays a main role in all three stages of unconventional methods containing drilling, production, and completion [1-3]. During the oil and gas production process, water which was injected into the well and the water produced from the well brought out of the well, and also, some amounts of water which has been trapped in reservoir rocks, are called produced water [4]. That's a very large volume of the wastewater which needs to be managed for treatment or other uses [5,6].

Produced water is the abundant and vast volume of wastewater in the petroleum and gas sectors [7,8]. There are several types of produced water according to their nature; they are from natural gas, oil and coal bed based according to their source and origin [9]. Note that the water composition changes from one well to another and even in a specific well over time [10].

Normally produced water contains a high concentration of heavy metals such as lead, barium, uranium, and cadmium, which are toxic for the environment and humans [11]. Moreover, due to the high concentration of different salts in the produced water, it is very salty and contains many suspended and dissolved solids [12, 13]. When the age of a well increases, normally the production of the well declines and the requirement for injection of water and furthermore the amount of produced water will be increased [14].

It is very interesting that the amount of produced water which comes out from a reservoir is around 98% in an old well with just 2% fossil fuel. It is anticipated that, by the aging of the oil and gas wells, the quantity of produced water would be increased in oil as well as gas wells and so it causes a high amount of wastewater and the environmental problems associated with that [15,16]. As the term "produced water" is utilized for the water associated with the produced oil and gas in the reservoir, it has different types. Produced water from different processes has different characteristics. For instance, produced water which is produced from the gas field is more toxic than the oilfield produced water. That is due to the high amount and concentration of aromatic contents such as toluene, xylene, and benzene [13,17].

Due to the large amount of produced water and high toxicity, it cannot be disposed simply into the environment. Furthermore, one of the main considerations in the oil industry is how to treat or reuse the produced water to be safe for disposal or other purposes such as irrigation. There are several methods for treatment of wastewaters and specially produced water (such as membrane treatment, thermal method, chemical treatment, sludge treatment) [18], but due to the huge amount of produced water, these methods have no any economic feasibility. Recently, due to the many global concerns on the environment, treatment of the produced water is very important; meanwhile, management of this large amount of wastewater and different steps of treatment and total cost make the well unprofit-

†To whom correspondence should be addressed.
E-mail: sedighi@qom.ac.ir, MBaboli@su.edu.om

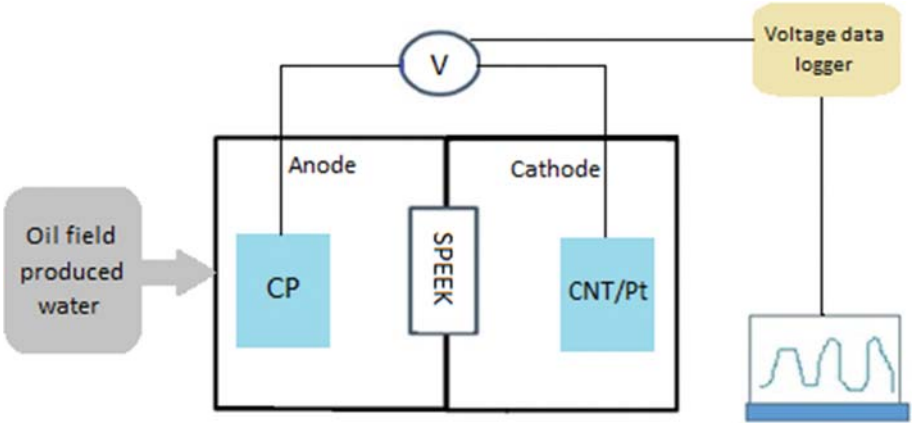

Fig. 1. Schematic of the MFC.

able [19].

Currently, biofuel cells and more especially MFC get high attention due to some precious advantages. They can treat the wastewater and also at the same time produce renewable energy [20,21].

Also, the only byproduct of this process is water [22,23]. MFC consists of two chambers which have been separated by a proton exchange separator [24]. Microorganisms in the anode degrade the feed which is produced water here and generate electrons and protons [25]. By utilization of organic substrate in the anode, the COD amount declines and electrons and protons will be generated, which can produce electricity [25].

Some studies before that have been done in simultaneous wastewater treatment along with energy production. In 2011, our group (Ghasemi et al.) replaced Pt with carbon nanofiber as a cathode catalyst in MFC due to high cost of Pt as a cathode catalyst [26]. We found that, by using carbon nanofiber as cathode catalyst, the amount of produced energy declined compared to the MFC which uses Pt as cathode catalyst, but on the other hand, the carbon nanofiber catalyst is more economically viable than Pt. The problem of using carbon nanofiber is its durability, which is very short specially when it is activated by some acidic agent. In another study, Zhang et al. [27], applied nitrogen-doped carbon nanotube as the support for Pt catalyst. They have found that the composite catalyst showed high efficiency compared to the Pt catalyst. They investigated that nitrogen content could help for better dispersion of Pt nanoparticles, which caused better catalytic activity. Moreover, nanotube itself opened up many networks around the active catalyst. Despite, it reduced the amount of Pt as a noble and expensive metal as the catalyst for oxygen reduction reaction (ORR) application.

As the Pt as cathode catalyst and Nafion 117 as the separator are the main obstacles of the viability of MFC, in this study, we used a CNT/Pt nanocomposite as cathode catalyst to reduce the amount of Pt and SPEEK as the separator (instead of Nafion 117) in MFC for treatment of produced water along with a lower capital cost. Also, the system produced electricity as a clean source of energy, which is environmentally friendly and does not pollute the atmosphere. Moreover, RSM was used to evaluate systematically and optimize the interactions of different parameters on the COD removal as well as power generation.

MATERIALS AND METHODS

1. MFC Configuration

The MFC used in this study has two cubic chambers with a volume of 600 cm^3 (10 cm, 6 cm, 10 cm) but with the working volume of 70% of its total volume means about 420 cm^3. SPEEK with various DS separated these two chambers used as proton exchange membrane (PEM). Oxygen was fed continuously to the cathode as an electron acceptor. The electrode has a surface area of 12 cm^2 in the anode and cathode. Fig. 1 shows a schematic of the MFC. The bacteria converted the organic substrate to the electrons and protons in an anaerobic environment of the anode. Then the electrons were transferred to the cathode from the external circuit and protons passed through the PEM. In the cathode, ORR occurred which produced electricity (O_2) and water (H_2O) and the amount of produced voltage was measured by a data logger which is linked to a computer.

2. Preparation of PEM

A representative sample of 30 g of poly ether ether ketone (PEEK) should be submerged in 500 ml of H_2SO_4 at room temperature and moved firmly for 1 h. For getting higher DS, the temperature must be increased up to 70 °C and 2-6 hours of stirring. More details about that method have been reported in our previous study [28].

3. CNT/Pt Electrode

For synthesizing CNT/Pt, a chemical reduction technique has been used. First, CNT was mixed with nitric acid in ultrasound. Next, the sample was collected and washed out with deionized water and then air dried. Again the sample should ultrasonicated with propanone for 1hour and the 0.75 M solution of H_2PtCl_6 solution added gradually. The sample should be reduced by 1 M sodium hydroxide as well as 0.1 M sodium borohydride [29].

4. Feed

Anode was fed by oilfield produced water from Malays Basin which was collected from Petronas Carigali, Malaysia. The representative sample was at separator from the Angsi field placed at offshore Terengganu, Malaysia. Produced water has was filtered by a simple paper before use as feed in the anode [30].

5. Analysis and Calculations

The X-ray diffraction (XRD) profile was acquired using an auto-

Table 1. Input variables and their corresponding ranges used by CCD

Variables	Symbols	Levels				
		$-\alpha$	−1	0	+1	$+\alpha$
DS of SPEEK[a]	X_1	10	20.25	45	69.75	80
Nanocomposite composition	X_2[b]	0	0.15	0.5	0.85	1

[a]DS of SPEEK or DS

[b]Factor X_2 was defined as $(1-X_2)$CNT/(X_2) Pt

mated powder diffractometer (Rigaku Dmax-2400, Japan). Scanning electron microscopy (SEM) (Supra 55vp-Zeiss, Germany) was performed to note the cross-section of the membrane together with the microorganism attachments on the anode surface. Moisture was eliminated until an essential level by dewatering the mix of produced water and the culture. Later, the specimen was covered with about 20-50 nm of carbon or gold, which operated as a conductive layer to facilitate the SEM test to be performed. Transition electronic microscopy (TEM, Philip, class CM12, Netherlands) was used for looking at Pt nanoparticle dispersion on the surface of the carbon nanotube.

To evaluate the COD, the samples were diluted ten times and 2 ml of the dilute mixture blended with a digestion solution having a wide range of COD. This was next heated at 150 °C in a Thermo reactor (Hach, DRB 200) and read with a spectrophotometer (Hach, DR 2800). The voltage was evaluated via a multimeter (Fluke, 8846A), and the power density (P) curve was calculated using power to the system at various loads. The current was calculated using the following equation:

$$I=\frac{V}{R} \tag{1}$$

where V is the voltage (volt), I is the current (amps), and R is the external resistance (ohm).

Subsequently, the P was measured by the formula:

$$P=R\times I^2 \tag{2}$$

The coulombic efficiency (CE) was measured as the current over time, as long as the most theoretical current was gained. The measured CE was computed by the following formula:

$$CE=\frac{M\int_0^t Idt}{FbV_{an}\Delta COD} \tag{3}$$

where F is faraday's constant, M is the molecular weight of oxygen, b=4 indicating the number of electrons exchanged per mole of oxygen, ΔCOD is the change in COD over time, 't' and V_{an} is the volume of liquid in the anode compartment, and entire the experiments were repeated three times and the average amounts were recorded.

6. Degree of Sulfonation (DS)

For finding the DS, 2-5% of SPEEK polymer solution was dissolved in the dimethyl sulfoxide (DMSO) solution and then evaluated under ^{1}H nuclear magnetic resonance (NMR) spectroscopy at 111 600 MHz via a cryoprobe (FT-NMR Advance, Bruker, Karlsruhe, Germany), to find the DS. The DS was derived by computing the ratio of distinct A_{H_E} to $A_{H_{A,A',B,B',C,D}}$ using the formula below [31]:

$$\frac{A_{H_E}}{\sum A_{H_{A,A',B,B',C,D}}}=\frac{n}{12-2n},\quad 0\le n\le 1 \tag{4}$$

where DS=n×100.

7. Design of Experimental Study

Once the intervals of each variable have been selected, the number and specific conditions of each variable have been specified by CCD, which is very effective since it supplies an even distribution of the empirical points [32,33]. According to our prior research, two main operating parameters, including DS (X_1) and nanocomposite composition (X_2), were selected as the variables. The reason for choosing these two parameters is their importance in the commercial viability of MFC and also their role in the efficiency of the MFC. It should be remarked that factor X_2 was determined as $(1-X_2)$ CNT/(X_2) Pt. For instance, Pt NP and 0.1CNT/0.9Pt nanocomposite were achieved at X_2=1 and X_2=0.9, respectively. These factors along with their values are outlined in Table 1.

A quadratic polynomial model, with linear, quadratic, and interaction terms, was supposed to relate the factors to the responses as follows:

$$Y=\beta_0+\beta_1X_1+\beta_2X_2+\beta_3X_3+\beta_{12}X_1X_2+\beta_{13}X_1X_3+\beta_{23}X_2X_3+\beta_{11}X_1^2+\beta_{22}X_2^2+\beta_{33}X_3^2+\varepsilon \tag{5}$$

where Y is the experimental response, X_i are the independent variables, β_0 is the intercept, β_i are the true coefficients, and ε is the experimental error.

To evaluate the model's appropriateness, analysis of variance (ANOVA) was carried out [34,35]. The coefficient of determination (R^2) was the main parameter used for model evaluation [36]. As R^2 is closer to 1, the finding results by the model will be more precise. *F*-value (Fisher variation ratio), probability value (*p*-value), and adequate precision (AP) are tools for assessing the quality and relevance of the model [37].

RESULTS AND DISCUSSION

1. Attachment of Microorganisms on the Electrode, SEM and TEM of CNT and CNT/Pt

Fig. 2(a) and 2(b) show the attachment of microorganisms to the surface of the anode electrode. As can be seen clearly, various types of microorganisms have been linked to the electrode surface. They act as biocatalyst and oxidize the organics of the feed which is found in oilfield water [38]. By oxidizing the feed, they produced electrons and protons for power generation. Fig. 2 also revealed

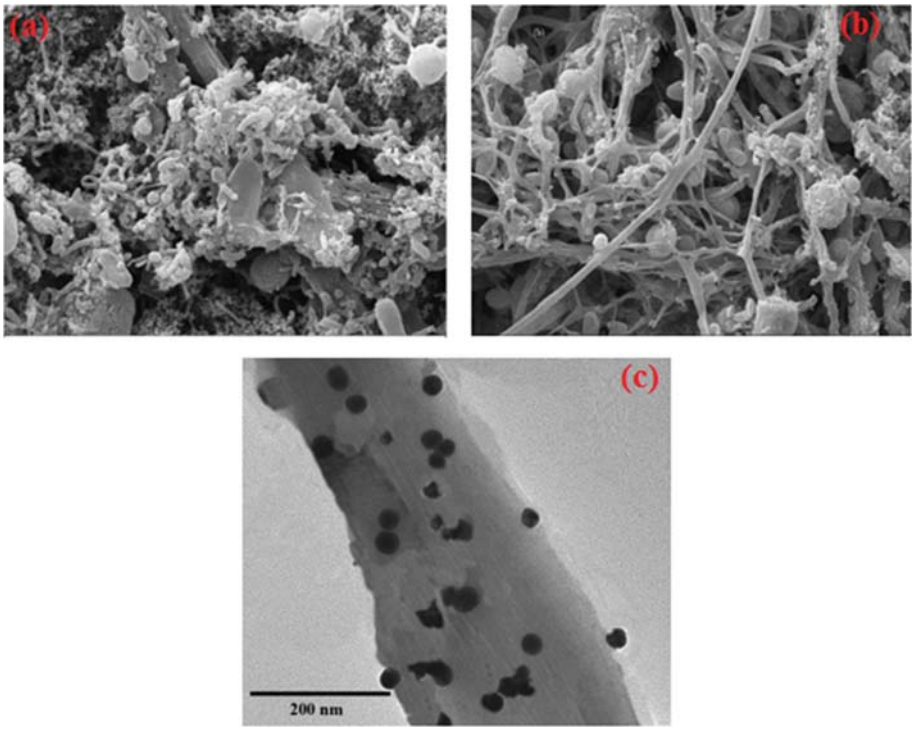

Fig. 2. (a), (b) SEM images from the attachment of mixed culture bacteria on the surface of the electrode. (c) TEM image of carbon nanotube (CNT)/Pt.

that the microorganisms have a very high affinity to the surface of the electrode and they fully covered the anode surface, which can be a good sign for utilizing the organic substrates on the produced water that has been used as the feed. Fig. 2(c) shows the distribution of the Pt particles on the CNT surface. As the figure clarifies, the Pt particles were distributed uniformly and were not accumulated on the surface of the CNT; this gives the opportunity for the proton to sit on the area of CNT and go through the ORR process.

2. Evaluation of DS by NMR

H_{13} NMR was analyzed to evaluate the DS for SPEEK (Fig. 3). SO_3H group intensity is shown in H_{13}. The intensity of H_{13} is equal to the content of the SO_3H band. The non-sulfonated groups are shown in 7.27 ppm in the graph obtained from the instrument. At the sulfonic functional groups, the process of the sulfonation of the PEEK has happened that caused the production of three types of protons (H_{13}, H_{14}, and H_{15}). The calculated DS was obtained from the equation according to the different SPEEK which has been used as a separator.

3. XRD Analysis

Fig. 4 displays the XRD analysis of the cathode electrode. The carbon nanotube peaks in 25.8° and 42.75° are the same as our previous studies [28,29]. The wide peaks that can be seen in 25.8° and smaller intensity in 42.75° reveal the well-resolved diffraction of the nanotube. As can be observed, the turbo static nature of well-dispersed nanotube has been clarified in 42.75 degrees of CNT/Pt peak. It is clearly bigger than CNT. The peak on the 61.58 which is quite sharp is necessary for the support of Pt on carbon nanotube as a catalyst [39].

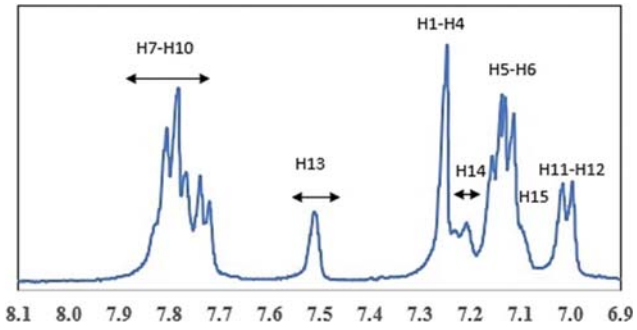

Fig. 3. NMR analysis of a sample of SPEEK.

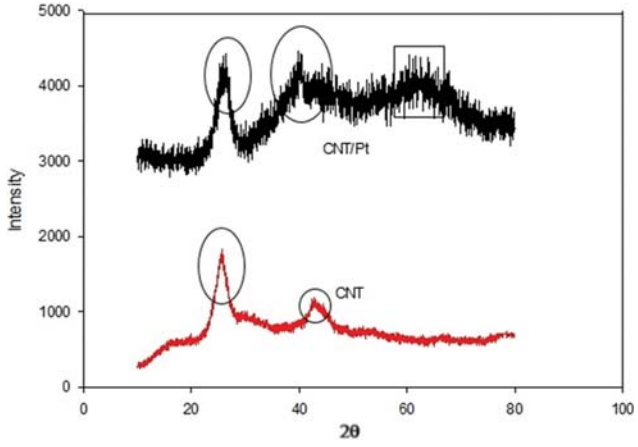

Fig. 4. XRD patterns of the carbon nanotube (CNT) and CNT/Pt.

Table 2. The corresponding experimental conditions and obtained responses

Run	Variables		Responses	
	X_1: DS	X_2: Nanocomposite composition	COD removal (%)	Power generation (mW/m^2)
1	45.00	0.50	48	365
2	69.75	0.15[a]	51	190
3	45.00	0.50	45	361
4	80.00	0.50	78	486
5	45.00	0.50	47	366
6	20.25	0.15	68	150
7	10.00	0.50	35	175
8	45.00	0.00	64	140
9	45.00	1.00	59	275
10	20.25	0.85	45	238
11	69.75	0.85	84	510

[a]For example, 0.15 was defined as 0.85CNT/0.15 Pt or 85 wt% CNT/15 wt% Pt

Table 3. Analysis of variance for the responses

Source	DF[a]	Sum of squares	Mean square	*F*-value	*p*-Value
For COD removal (R^2=0.89)					
Model	5	2,084.80	416.96	8.43	0.0177
Residual	5	247.38	49.48		
Lack of fit	3	242.72	80.91	34.67	0.0282
Pure error	2	4.67	2.33		
Total	10	2,332.18			
For power generation (R^2=0.95)					
Model	5	163,200	32,630.24	20.48	0.0024
Residual	5	7,964.79	1,592.96		
Lack of fit	3	7,950.79	2,650.26	378.61	0.0026
Pure error	2	14.00	7.00		
Total	10	171,100			

[a]DF: Degree of freedom.

4. Statistical Analysis and Modelling using RSM

Table 1 in the experiment section was conducted for two specific independent system parameters and their dynamic interaction was examined on percentage removal of COD and power generation. The results are presented in Table 2.

The relation between variables and responses was analyzed using the second-order polynomial formula as follows:

$$\text{COD removal (\%)} = +89.246 - 1.214X_1 - 136.298X_2 + 1.600X_1X_2 + 0.00925X_1^2 + 65.333X_2^2 \quad (6)$$

$$\text{Power (mW/m}^2) = +28.493 + 2.834X_1 + 533.464X_2 + 6.628X_1X_2 - 0.026X_1^2 - 620X_2^2 \quad (7)$$

The ANOVA guarantees a good model. The ANOVA analysis of the proven RSM model presented *F*-values of 8.43 for COD removal and 20.48 for power generation, suggesting that the model was significant (Table 3). The R^2 amount of 0.89 was noted for COD removal. Nevertheless, the R^2 value of 0.95 was observed for power generation, thus indicating a close correlation between the expected model and the performance factors (Table 3). Also, the AP was 9.375 and 13.374 for the final models of COD removal and power generation, which measure the signal to noise ratio. A ratio >4 is appropriate. The ratio of 9.375 and 13.374 indicates an appropriate signal. So, this model can be utilized to manage the design space.

The predicted and experimental values of COD removal and power are presented in Fig. 5(a) as well as 5(b), respectively. In Fig. 5, the distribution of actual values is close to a straight line, indicating the good fitness of the model.

4-1. Perturbation Plots

The individual effect of variables DS (X_1) and nanocomposite (X_2) on COD removal as well as power generation was found by the perturbation plot (Fig. 6). This diagram reflects a general view of the effect of altering the parameters on the result. As shown in Fig. 6(a) and 6(b), variables X_1 and X_2 were very sensitive to COD removal and power generation. The graphs showed that always with increasing the DS, the power generation and COD removal would be increased. It may due to the pH of the anode that once is in neutral range and the transport of protons to the cathode increases, the pH is in the range that bacteria keep their activity as well as by being transferred to the cathode, they also engaged in

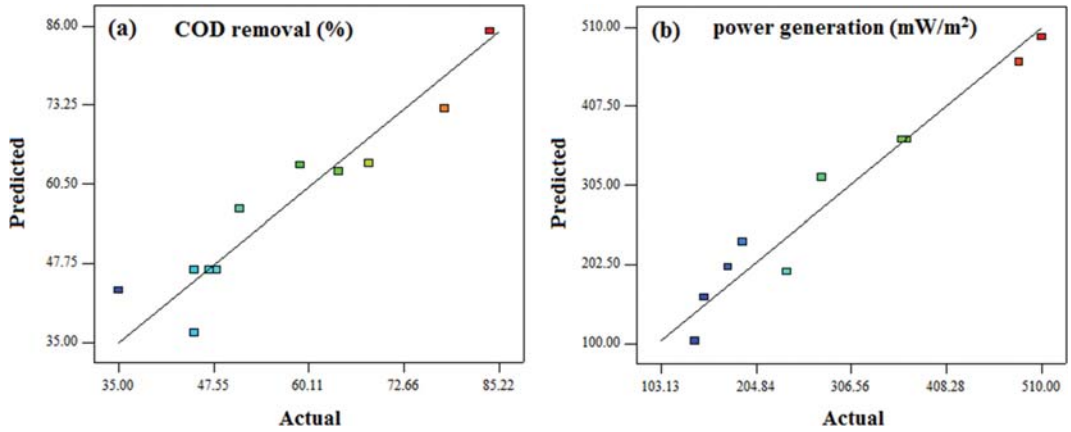

Fig. 5. Plots of predicted versus actual values, (a) COD removal, and (b) power generation.

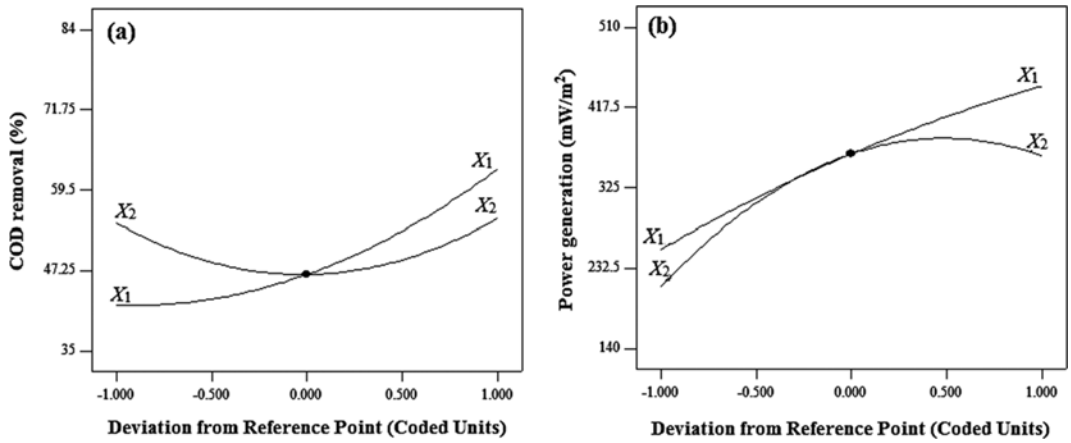

Fig. 6. Perturbation plot showing the simultaneous effect of parameters.

power generation [40,41].

But the trend for the nanocomposite is quite different. It increases slightly to 14% and after that declines. This effect is most probably is due to the fact that, however the CNT causes the surface area increment, but this is not enough for ORR and it needs a catalyst such as Pt for reduction of protons. However, even 14% composition of CNT in the CNT/Pt could be a great finding for reduction of the amount of Pt as an expensive catalyst [42,43].

4-2. Combination Result of Operating Parameters for COD Removal (%) and Power Generation

The response surface and two-dimensional contour plots for COD removal as well as power generation versus DS and nanocomposite are shown in Fig. 7(a)-(c). At low nanocomposite composition, COD removal decreased with the increase of DS (Fig. 7(a), (b)) and then, COD removal increased with higher DS (Fig. 7(a), (b)), which might be due to indirect effect of SPEEK as the PEM. When the separator exchanges a higher amount of proton in the anode, the pH in the anode chamber stays more near neutral and so the mixed culture bacteria have more capability for utilizing the organic sources of the anode [44].

At high nanocomposite composition, the percentage of COD removal improved to 91% with the increase in the DS (Fig. 7(a), (b)). Because, as the organic source of the anode, have been consumed and the electrons and protons in different ways reached the cathode part, the proton needs to be absorbed on the cathode and reduced by ORR [45-47]. The source of oxygen is from the anode part. Higher nanocomposite percentage offered higher surface area and place for ORR compared to the composite cathode. One of the characteristics of nanomaterials and nanocomposite is providing higher surface area and then higher catalytic activity [48,49].

Fig. 7(c) and (d) show the effects of nanocomposite composition and DS on the power generation. It can be confirmed by Fig. 7(c) and (d) that at high DS, the power generation increased when the nanocomposite composition increased from 0 to 0.86 but reduced slightly when the nanocomposite composition was improved from 0.86 to 1. This may be because there is not enough space and position for the ORR in the pure platinum catalyst [50].

4-3. Optimization

One of the key objectives of this study was to achieve the optimum requirements for COD removal as well as power generation from oilfield produced water. The findings were optimized using the CCD-based RSM regression formula [51]. The optimization of DS (X_1) and nanocomposite composition (X_2) were identified within range and the responses including COD removal (Y_1) as well as power generation (Y_2) were maximized. Under these optimal operating conditions such as DS (X_1)=80 with nanocomposite composi-

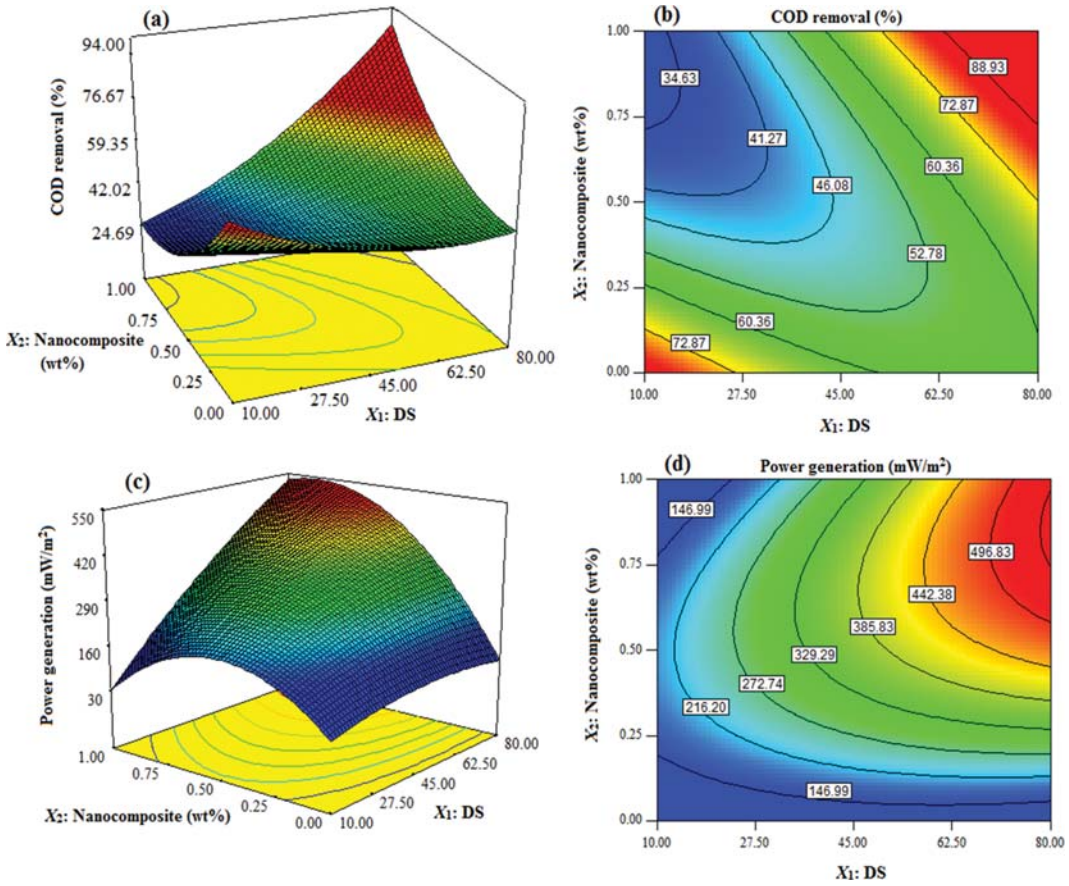

Fig. 7. Response surface plots of ((a), (b)) COD removal, and ((c), (d)) power generation.

Table 4. Experimental and predicted power generation and COD removal of produced water treatment in MFC under optimal operating conditions

Responses	Model	Experimental	Relative error
Power generation (mW/m^2)	545.05	540.11	0.91%
COD removal (%)	92.51	91.28	1.33%

tion (X_2)=0.86 (14 wt% CNT-86 wt% Pt), the percentage removal of COD as well as power generation were found to be 92.51% and 545.05 mW/m^2, respectively. The experimental run was carried out with the parameters set at optimum conditions and the COD removal and power generation were observed at 91.28% and 540.11 mW/m^2, respectively, in good agreement with the expected values obtained (Table 4).

Also, the CE of the MFC system in a different situation and designed experiments have been calculated. The CE means the percentage of the feed that would be converted to electricity. The highest CE 72% belonged to the optimized condition with DS=80 and the catalyst of 14 wt%-CNT and 86 wt%-Pt. The interesting result belongs to the MFC with DS=45 and full platinum cathode, which has the CE of 40% with the power generation of 275 mW/m^2 and COD removal of 59%, which has the middle power generation and COD removal compared to other cases. It can be due to the fact that, CE means what percentage the produced electrons and protons converted to electricity. And the MFC with the DS=45 and full platinum catalyst due to having a proper situation in media and cathode such as pH and the anolyte's conductivity could be able to convert them to the electricity. One more result that can be found from the graphs is that the optimized composition of the nanocomposite catalyst could be able to convert more electrons to the electricity, while the conventional pure Pt electrode had lesser performance in producing electricity with the same feed. Also, because the experiments were conducted in three months, the durability of the cathode is an issue which directly influences the performance [52,53].

CONCLUSION

In this study, we treated a vast source of wastewater by an environmentally friendly method and also generated electricity.

a) The RSM results clarified significant effects of the variables including DS and nanocomposite composition (CNT/Pt) along with their interactive impact on the COD removal and power genera-

tion by MFC.

b) High R^2 values for all ANOVA models suggested that the reliability of the polynomial model was appropriate.

c) A multiparameter optimization was performed with two factors. The RSM optimization confirmed that the experimental data were well matched to the quadratic models for COD removal and power generation.

d) The results showed that MFC could remove 92% of COD and generate 545 mW/m^2 of power density at optimum conditions of DS=80 and nanocomposite composition of 0.86 (14 wt% CNT-86 wt% Pt). The highest CE also belongs to this situation with 72%.

e) It was found that, by making a nanocomposite catalyst, a lower amount of Pt could be used and so MFC became more economical. It opened up a new window to reduce the amount of Pt as the common catalyst by making a nanocomposite catalyst.

f) For future research, some pre-treatments should be applied on produced water before treatment by MFC. That is obvious that, due to the complex structure of produced water, breaking down the carbon sources as the feed in the anode is difficult even for the mixed culture of bacteria.

ACKNOWLEDGEMENT

The authors would like to express their sincere appreciation to the Chemical Engineering Section at the Faculty of Engineering of the Sohar University of Oman for their kind supports.

NOMENCLATURE

A_{H_E} : peak area of the different H_E signal
$A_{H_{A,A',B,B',C,D}}$: peak area of the signals corresponding to all the other aromatic hydrogen
ANOVA : analysis of the variance
AP : adequate precision
b : number of electrons exchanged per mole of oxygen
CCD : central composite design
CE : coulombic efficiency
COD : chemical oxygen demand
DF : degree of freedom
DS : degree of sulfonation
F : Faraday's constant
F-value : fisher variation ratio
I : current [amps]
M : molecular weight of oxygen
MFC : microbial fuel cell
n : number of H_E per repeat unit
ORR : oxygen reduction reaction
P : power density
PEM : proton exchange membrane
PEEK : poly ether ether ketone
p-value : probability value
R : external resistance [ohm]
R^2 : coefficient of determination
RSM : response surface methodology
SPEEK : sulfonated poly ether ether ketone
V : voltage [volt]
V_{an} : volume of liquid in the anode compartment
ΔCOD : change in COD over time, 't'

REFERENCES

1. J. Hao, S. Mohammadkhani, H. Shahverdi, M. N. Esfahany and A. Shapiro, *J. Pet. Sci. Eng.*, **179**, 276 (2019).
2. K. Subramanian, T. N. Rao and A. Balakrishnan, *Nanofluids and their engineering applications*, 1st Ed., CRC Press, Boca Raton (2019).
3. M. Safari, M. Mohammadi and M. Sedighi, *J. Appl. Geophy.*, **138**, 33 (2017).
4. A. Agi, R. Junin, A. Y. M. Alqatta, A. Gbadamosi, A. Yahya and A. Abbas, *Ultrason. Sonochem.*, **51**, 214 (2019).
5. H. Chang, T. Li, B. Liu, R. D. Vidic, M. Elimelech and J. C. Crittenden, *Desalination*, **455**, 34 (2019).
6. S. Munirasu, M. A. Haija and F. Banat, *Process Saf. Environ. Prot.*, **100**, 183 (2016).
7. M. A. Al-Ghouti, M. A. Al-Kaabi, M. Y. Ashfaq and D. A. Da'na, *J. Water Process Eng.*, **28**, 222 (2019).
8. G. Ji, T. Sun, Q. Zhou, X. Sui, S. Chang and P. Li, *Ecol. Eng.*, **18**, 459 (2002).
9. S. Jiménez, M. Micó, M. Arnaldos, F. Medina and S. Contreras, *Chemosphere*, **192**, 186 (2018).
10. A. Fakhru'l-Razi, A. Pendashteh, L. C. Abdullah, D. R. A. Biak, S. S. Madaeni and Z. Z. Abidin, *J. Hazard. Mater.*, **170**, 530 (2009).
11. M. Wang, M. Wang, D. Chen, Q. Gong, S. Yao, W. Jiang and Y. Chen, *J. Environ. Chem. Eng.*, **7**, 102878 (2019).
12. H. Fakharian, H. Ganji and A. Naderifar, *J. Taiwan Inst. Chem. Eng.*, **72**, 157 (2017).
13. P. Jain, M. Sharma, P. Dureja, P. M. Sarma and B. Lal, *Chemosphere*, **166**, 96 (2017).
14. B. Jia, *J. Taiwan Inst. Chem. Eng.*, **104**, 82 (2019).
15. J. Zheng, B. Chen, W. Thanyamanta, K. Hawboldt, B. Zhang and B. Liu, *Mar. Pollut. Bull.*, **104**, 7 (2016).
16. C. Wang, Z. Wang, X. Wei and X. Li, *J. Water Process Eng.*, **32**, 100972 (2019).
17. G. Mohanakrishna, R. I. Al-Raoush, I. M. Abu-Reesh and K. Aljaml, *Sci. Total Environ.*, **665**, 820 (2019).
18. H. Li, J. Watson, Y. Zhang, H. Lu and Z. Liu, *Bioresour. Technol.*, **298**, 122421 (2019).
19. E. T. Igunnu and G. Z. Chen, *Int. J. Low-Carbon Tech.*, **9**, 157 (2014).
20. C. M. Jeong, J. D. R. Choi, Y. Ahn and H. N. Chang, *Korean J. Chem. Eng.*, **25**, 535 (2008).
21. N. T. Trinh, J. H. Park, S. S. Kim, J.-C. Lee, B. Y. Lee and B.-W. Kim, *Korean J. Chem. Eng.*, **27**, 546 (2010).
22. M. Ghasemi, W. R. W. Daud, A. F. Ismail, Y. Jafari, M. Ismail, A. Mayahi and J. Othman, *Desalination*, **325**, 1 (2013).
23. M. Sedighi, S. A. Aljlil, M. D. Alsubei, M. Ghasemi and M. Mohammadi, *Alex. Eng. J.*, **57**, 4243 (2018).
24. Z. Najafgholi and M. Rahimnejad, *Korean J. Chem. Eng.*, **33**, 154 (2016).
25. J. X. Leong, W. R. W. Daud, M. Ghasemi, K. B. Liew and M. Ismail, *Renew. Sust. Energy Rev.*, **28**, 575 (2013).
26. M. Ghasemi, S. Shahgaldi, M. Ismail, B. H. Kim, Z. Yaakob and W. R. W. Daud, *Int. J. Hydrogen Energy*, **36**, 13746 (2011).
27. L.-M. Zhang, X.-L. Sui, L. Zhao, J.-J. Zhang, D.-M. Gu and Z.-B.

Wang, *Carbon*, **108**, 561 (2016).
28. M. Ghasemi, W. R. W. Daud, J. Alam, Y. Jafari, M. Sedighi, S. A. Aljlil and H. Ilbeygi, *Int. J. Hydrogen Energy*, **41**, 4862 (2016).
29. M. Ghasemi, M. Ismail, S. K. Kamarudin, K. Saeedfar, W. R. W. Daud, S. H. Hassan, L. Y. Heng, J. Alam and S.-E. Oh, *Appl. Energy*, **102**, 1050 (2013).
30. S. Hisham, F. A. Khan, S. A. Aljlil and M. Ghasemi, *SN Appl. Sci.*, **1**, 646 (2019).
31. H. Ilbeygi, A. Mayahi, A. Ismail, M. Nasef, J. Jaafar, M. Ghasemi, T. Matsuura and S. Zaidi, *J. Taiwan Inst. Chem. Eng.*, **45**, 2265 (2014).
32. D. C. Montgomery, *Design and analysis of experiments*, Wiley, United States (2017).
33. M. Sedighi, M. Mohammadi, M. Sedighi and M. Ghasemi, *Energy Fuels*, **32**, 7412 (2018).
34. M. Mohammadi, M. Sedighi and V. Alimohammadi, *Int. J. Nano Dimens.*, **10**, 195 (2019).
35. M. Nouri, M. Sedighi, M. Ghasemi and M. Mohammadi, *Korean J. Chem. Eng.*, **30**, 1700 (2013).
36. M. Mohammadi, M. Dadvar and B. Dabir, *J. Mol. Liq.*, **238**, 326 (2017).
37. F. Momtazan, A. Vafaei, M. Ghaedi, A. M. Ghaedi, D. Emadzadeh, W.-J. Lau and M. M. Baneshi, *Korean J. Chem. Eng.*, **35**, 1108 (2018).
38. M. Ghasemi, A. M. Nassef, M. Al-Dhaifallah and H. Rezk, *Int. J. Energy Res.*, **1**, 1 (2020).
39. M. Ghasemi, W. R. W. Daud, S. H. Hassan, T. Jafary, M. Rahimnejad, A. Ahmad and M. H. Yazdi, *Int. J. Hydrogen Energy*, **41**, 4872 (2016).
40. Y. Mohan and D. Das, *Int. J. Hydrogen Energy*, **34**, 7542 (2009).
41. B. Hou, J. Sun and Y.-y. Hu, *Bioresour. Technol.*, **102**, 4433 (2011).
42. N. Garino, A. Sacco, M. Castellino, J. A. Muñoz-Tabares, A. Chiodoni, V. Agostino, V. Margaria, M. Gerosa, G. Massaglia and M. Quaglio, *ACS Appl. Mater. Interfaces*, **8**, 4633 (2016).
43. A. Mehdinia, E. Ziaei and A. Jabbari, *Electrochim. Acta*, **130**, 512 (2014).
44. A. Kongkanand and M. F. Mathias, *J. Phys. Chem. Lett.*, **7**, 1127 (2016).
45. H. S. Ahn and T. D. Tilley, *Adv. Funct. Mater.*, **23**, 227 (2013).
46. J. An, H. Jeon, J. Lee and I. S. Chang, *Environ. Sci. Technol.*, **45**, 5441 (2011).
47. B. Erable, D. Féron and A. Bergel, *ChemSusChem*, **5**, 975 (2012).
48. T. Chen and L. Dai, *Mater. Today*, **16**, 272 (2013).
49. A. H. Khan, S. Ghosh, B. Pradhan, A. Dalui, L. K. Shrestha, S. Acharya and K. Ariga, *Bull. Chem. Soc. Jpn.*, **90**, 627 (2017).
50. C. Baldizzone, S. Mezzavilla, H. W. Carvalho, J. C. Meier, A. K. Schuppert, M. Heggen, C. Galeano, J. D. Grunwaldt, F. Schüth and K. J. Mayrhofer, *Angew. Chem. Int. Ed.*, **53**, 14250 (2014).
51. M. Sedighi and M. Mohammadi, *J. CO2 Util.*, **35**, 236 (2020).
52. M. Gummalla, S. C. Ball, D. A. Condit, S. Rasouli, K. Yu, P. J. Ferreira, D. J. Myers and Z. Yang, *Catalysts*, **5**, 926 (2015).
53. H. Yano, M. Watanabe, A. Iiyama and H. Uchida, *Nano Energy*, **29**, 323 (2016).